# Protein phosphatase 5 is a negative regulator of separase function during cortical granule exocytosis in *C. elegans*

**Christopher T. Richie[1,*,‡], Joshua N. Bembenek[2,‡,§], Barry Chestnut[1,¶], Tokiko Furuta[3], Jill M. Schumacher[3], Matthew Wallenfang[4] and Andy Golden[1,**]**

[1]Laboratory of Biochemistry and Genetics, NIDDK, NIH, Bethesda, MD 20892, USA
[2]Laboratory of Molecular Biology, University of Wisconsin-Madison, Madison, WI 53706, USA
[3]Department of Genetics, University of Texas, M. D. Anderson Cancer Center, Houston, TX 77030, USA
[4]Department of Biological Sciences, Barnard College, New York, NY 10027, USA

*Present address: Neural Protection and Regeneration Branch, NIDA, Baltimore, MD 21224, USA
‡These authors contributed equally to this work
§Present address: Department of Molecular, Cellular and Developmental Biology, University of Michigan, Ann Arbor, MI 48109-1048, USA
¶Present address: Mammary Biology and Tumorigenesis Laboratory, NCI, Bethesda, MD 20892, USA
**Author for correspondence (andyg@mail.nih.gov)

*Accepted 3 May 2011*
*Journal of Cell Science 124, 2903–2913*

*doi: 10.1242/jcs.073379*

## Summary

Mutations in the *Caenorhabditis elegans* separase gene, *sep-1*, are embryonic lethal. Newly fertilized mutant embryos have defects in polar body extrusion, fail to undergo cortical granule exocytosis, and subsequently fail to complete cytokinesis. Chromosome nondisjunction during the meiotic divisions is readily apparent after depletion of *sep-1* by RNAi treatment, but much less so in hypomorphic mutant embryos. To identify factors that influence the activity of separase in cortical granule exocytosis and cytokinesis, we carried out a genetic suppressor screen. A mutation in the protein phosphatase 5 (*pph-5*) gene was identified as an extragenic suppressor of *sep-1*. This mutation suppressed the phenotypes of hypomorphic separase mutants but not RNAi depleted animals. Depletion of *pph-5* caused no phenotypes on its own, but was effective in restoring localization of mutant separase to vesicles and suppressing cortical granule exocytosis and cytokinesis phenotypes. The identification of PPH-5 as a suppressor of separase suggests that a new phospho-regulatory pathway plays an important role in regulating anaphase functions of separase.

**Key words:** Separase, Cortical granule exocytosis, Protein phosphatase 5

## Introduction

The maintenance of the cohesin complex that holds newly replicated sister chromatids together through metaphase and its timely dissolution at the onset of anaphase are crucial for a successful mitotic cell division. The widely conserved protease, separase, cleaves the Scc1 (also known as Rad21) subunit of the cohesin complex, thereby allowing sister chromatids to be pulled apart towards the spindle poles at anaphase. Before the metaphase-to-anaphase transition, separase is held in an inactive conformation by an inhibitory chaperone, securin. Securin is ubiquitylated by the anaphase promoting complex or cyclosome (APC/C) and subsequently degraded by the proteasome, leading to the activation of separase at anaphase onset.

In addition to the canonical function of separase in cohesin cleavage, new evidence points to other anaphase functions for separase during the meiotic divisions. In murine oocytes, separase is required for the successful extrusion of polar bodies by an unknown mechanism (Kudo et al., 2006). The *Caenorhabditis elegans* separase, *sep-1*, was shown to have a role in the exocytosis of specialized vesicles known as cortical granules (CGs), which occurs during the first meiotic division (Bembenek et al., 2007). In addition to localizing to chromosomes and meiotic spindle, the SEP-1 protein can also be found on CG vesicle membranes before their fusion with the plasma membrane during anaphase of meiosis I.

Separase also regulates membrane trafficking during mitosis in *C. elegans* (Bembenek et al., 2010). SEP-1-depleted embryos fail to complete cytokinesis. Separase localizes to the ingressing cytokinetic furrow and regulates the incorporation of RAB-11-positive vesicles into the plasma membrane at the furrow. In human cell lines, both securin and separase regulate membrane traffic and protein secretion (Bacac et al., 2011). A genome-wide RNAi screen in a *Drosophila* cell line identified separase as a candidate required for constitutive protein secretion and Golgi organization (Bard et al., 2006). Therefore, separase controls membrane trafficking events in addition to its well-conserved role in cohesin cleavage.

The regulation of separase in membrane trafficking events in both mitotic and meiotic cells is currently under intensive investigation in a number of laboratories. Separase is inhibited by phosphorylation and Cdk1–cyclinB binding (Gorr et al., 2005) and thus securin is not the sole regulator of separase. Phosphorylation also regulates securin (Agarwal and Cohen-Fix, 2002) and the substrates of separase (Alexandru et al., 2001; Rogers et al., 2002). Although the canonical regulatory pathway is sufficient to ensure the timely onset of anaphase, phospho-

regulation of the separase pathway could be crucial for the coordinated regulation of cohesin cleavage and membrane trafficking.

In *C. elegans*, the *sep-1* gene is essential for embryonic viability partly because of its role in chromosome segregation (Siomos et al., 2001). Previously, the only allele known was *e2406ts*, a temperature-sensitive allele. Further analysis revealed that embryos with this allele have a significant reduction in the rate and overall number of CG exocytic events (Bembenek et al., 2007). Just after fertilization, chitin synthesis is initiated (Johnston et al., 2010). Next, during anaphase I, the contents of the CGs are released and assembled to form the impermeable eggshell (Sato et al., 2008). Hence the reduction of cortical granule exocytosis (CGE) in the *sep-1* mutant causes eggshell defects that result from insufficient proteoglycan secretion from CGs (Olson et al., 2006). The precise function of SEP-1 on these vesicles has yet to be determined. Importantly, homozygous *sep-1(e2406ts)* embryos show minimal chromosome segregation defects (Bembenek et al., 2007), although RNA interference (RNAi)-treated embryos do display this expected defect (Siomos et al., 2001). Furthermore, the SEP-1 protein in *sep-1(e2406ts)* mutants fails to localize to vesicles, yet still localizes to the spindle (Bembenek et al., 2007). These data suggest that *sep-1(e2406ts)* specifically affects the membrane trafficking functions of *sep-1*, making it a 'separation-of-function' allele.

Here we report the characterization of two novel *sep-1* alleles that produce defects in CGE (Bembenek et al., 2007) similar to the *sep-1(e2406ts)* mutant. Using the advanced genetics available in *C. elegans*, we identified mutations in the *pph-5* gene that function as suppressors of the embryonic lethality of separase mutants. The proteins encoded by these new separase alleles did not have the same subcellular localization as wild-type SEP-1 and these new *sep-1* alleles were not equally suppressed by mutations in the *pph-5* gene. Interestingly, the *pph-5* mutants restored the localization of SEP-1 mutant proteins to CGs. The *pph-5* mutants displayed no developmental defects in an otherwise wild-type background. Our work defines a novel regulatory mechanism involving the PPH-5 phosphatase, which regulates the CGE and cytokinesis activities of separase during anaphase. Given the numerous roles that phosphorylation plays in the regulation of separase activity and substrate susceptibility, our discovery of PPH-5 as a crucial regulator of separase reveals new insights into the phospho-regulation of the separase pathway in the early embryo of *C. elegans*.

## Results

### Characterization of mutant phenotypes of the novel *sep-1* alleles

We identified two novel alleles of the *C. elegans sep-1* gene, *ax110* and *ax521*, from a collection of mutants isolated in a temperature-sensitive embryonic lethal screen (Golden et al., 2000). Both these alleles failed to complement *sep-1(e2406ts)*; sequencing revealed that *ax110* and *ax521* are point mutations in separase that result in the amino acid changes H738P and C232Y, respectively (Fig. 1A). These *sep-1* alleles exhibited a recessive non-conditional maternal-effect lethal (Mel) phenotype that was fully penetrant at the non-permissive temperature of 24℃ (Table 1, lines 2 and 3) and >95% penetrant at 16℃ (data not shown). Unlike *sep-1(e2406ts)*, these two alleles did not cause sterility at any temperature. DAPI staining of embryos revealed a failure to extrude polar bodies (Fig. 1C); the resulting polyploid embryos continued to undergo sequential rounds of DNA replication without cytokinesis (Fig. 1E,F). The terminal phenotype was arrest as multinucleated one-cell embryos (Fig. 1C,E,F). Interestingly, all three alleles caused minimal chromosome segregation defects during the meiotic divisions (Fig. 2), unlike *sep-1* RNAi (Siomos et al., 2001), suggesting that cohesin cleavage during the meiotic divisions is normal. However, during mitosis (Fig. 1E,F; Fig. 2), lagging chromosomes and chromosome bridges were observed, but to a lesser degree than with *sep-1* RNAi. We believe that the chromosome segregation defects that we observed during mitosis in mutants with these alleles are due to the incorporation of abnormal chromatin, derived from failed polar body extrusion, into the metaphase plate. In cases where chromatin from failed polar body extrusion did not incorporate into the spindle, nondisjunction was much less severe (Fig. 2E–H; supplementary material Movie 1). Given that the *sep-1* mutations caused minimal meiotic chromosome segregation defects, but were much more penetrant for polar body extrusion and cytokinesis defects than strict loss of function by *sep-1* RNAi (Fig. 2Q–T), we conclude that these three *sep-1* alleles are probably separation-of-function alleles.

To more fully characterize the mitotic phenotypes of the new *sep-1* alleles, we analyzed embryos expressing GFP::histone

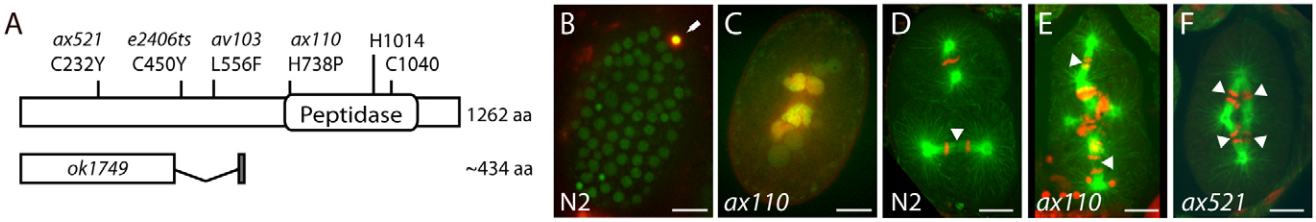


**Fig. 1. Novel *sep-1* mutants share osmotic sensitivity and cytokinesis defects but are competent for chromosome segregation.** (**A**) A schematic representation of the *C. elegans* SEP-1 protein denoting the locations of the amino acid substitutions encoded by the mutations *ax110*, *ax521* and *e2406ts*, as well as *av103*, the intragenic suppressor of *sep-1(e2406ts)*. The regions with corresponding homology to the separase ortholog pfam group (peptidase C50) and the catalytic histidine and cysteine residues are indicated. The truncated and frame-shifted protein predicted to be expressed from the *sep-1(ok1749)* allele is also shown. The shaded box represents the out-of-frame residues that are encoded before the premature stop codon. (**B**,**C**) In a live *sep-1(+)* embryo (B) only the first polar body (indicated by a white arrow) was stained by DAPI (yellow), whereas in a live *sep-1(ax110)* embryo (C), the polyploid zygotic DNA stained with DAPI. The embryos expressed GFP::histone to reveal zygotic DNA (green). (**D**–**F**) Methanol-fixed embryos stained with anti-tubulin antibodies (green) and TOTO-3 (red). (D) A two-cell wild-type embryo, (E) a 'four-cell' polyploid *ax110* embryo and (F) a 'two-cell' polyploid *ax521* embryo. The arrowheads indicate successful chromosome separation at anaphase. Scale bars: 10 μm.

**Table 1. Novel *sep-1* mutants exhibit a severe maternal effect lethal phenotype that can be suppressed by a reduction in *pph-5* activity**

| Strain at 24℃ (unless otherwise noted) | Total embryos | % Hatching |
|---|---|---|
| 1. N2 | 1954 | 99.7 |
| 2. *sep-1(ax110)* | 2284 | 0.0 |
| 3. *sep-1(ax521)* | 1505 | 0.0 |
| 4. *sep-1(e2406ts)* at 20℃ | 221 | 0.0 |
| 5. *sep-1(e2406ts)* | Sterile | NA |
| 6. *pph-5(av101)* | 1602 | 99.2 |
| 7. *sep-1(ax110); pph-5(av101)* | 2013 | 91.6 |
| 8. *sep-1(ax521); pph-5(av101)* | 1268 | 0.0 |
| 9. *sep-1(e2406ts); pph-5(av101)* at 20℃ | 3782 | 96.2 |
| 10. *sep-1(e2406ts); pph-5(RNAi)* at 20℃ | 196 | 69.9 |
| 11. *sep-1(e2406ts); pph-5(av101)* | Sterile | NA |
| 12. N2; *smd-1(RNAi)* | 514 | 100 |
| 13. *sep-1(ax110); smd-1(RNAi)* | 445 | 0.0 |
| 14. *pph-5(av101); smd-1(RNAi)* | 705 | 98.0 |
| 15. *sep-1(ax110); pph-5(av101); smd-1(RNAi)* | 905 | 93.1 |
| 16. N2; *pph-5(RNAi)* | 512 | 99.2 |
| 17. *sep-1(ax110); pph-5(RNAi)* | 498 | 72.3 |
| 18. *sep-1(ax110); pph-5(av101); pph-5(RNAi)* | 937 | 96.1 |
| 19. *pph-5(av101); pph-5(RNAi)* | 1236 | 99.5 |
| 20. *pph-5(tm2979)* | 2173 | 99.7 |
| 21. *pph-5(tm2979); pph-5(RNAi)* | 1293 | 98.8 |
| 22. *sep-1(ax110); pph-5(tm2979)* | 809 | 97.7 |
| 23. *sep-1(e2406ts); pph-5(tm2979)* at 20℃ | 797 | 97.9 |

*sep-1(e2406ts)* animals at their non-permissive temperature of 20℃ layed a brood of embryos that fail to hatch (line 4), but are suppressed by *pph-5(av101* or *tm2979)* at this temperature (lines 9 and 23). The *smd-1* gene was used as a negative control, as it has no obvious RNAi phenotype (lines 12–15).

Numbers in the second and third columns reflect the total progeny counted after pooling several experiments (with a minimum of five mothers per strain). Unsuppressed strains were maintained at 24℃ as heterozygotes balanced over the hT2 balancer chromosome. Homozygous L4 *sep-1* mutants were moved to new plates and embryonic viability and lethality were monitored daily.

H2B. At 25℃, 83% ($n$=5/6) of *sep-1(ax110)* embryos showed cytokinesis failures whereas only 50% ($n$=3/6) of the embryos showed chromosome bridges during mitotic anaphase (Fig. 2E–H,Q,R). Similar observations were made with *sep-1(ax521)* embryos (data not shown). By contrast, *sep-1* RNAi caused a higher incidence of more severe chromosome nondisjunction but fewer cytokinesis failures (Fig. 2I–L,Q,R) (Bembenek et al., 2010), consistent with the hypothesis that these new alleles are separation-of-function alleles. The homozygous *sep-1(ax110* and *ax521)* mutant progeny developed into fertile adults at all temperatures (16–25℃) in contrast to mutants with the conditional allele *e2406ts*, where homozygous animals developed into sterile uncoordinated (Stu) adults at temperatures above 20℃ (Table 1, lines 4 and 5) (Siomos et al., 2001). A deletion allele, *sep-1(ok1749)*, which removes a 1.2 kb region from within intron 3 to within exon 6 (Fig. 1) was predicted to cause aberrant splicing into sequences within exon 6. This would result in a frameshift that would encode a truncated SEP-1 protein without a protease domain. This protein is unstable as it was not detected by western blot analysis (supplementary material Fig. S1). Homozygous *sep-1(ok1749)* animals died during larval development or developed into Stu adults.

Loss of separase function causes a defect in CGE and eggshell formation (Bembenek et al., 2007; Siomos et al., 2001). Therefore, we tested whether the novel *sep-1* alleles also confer an eggshell phenotype. Live embryos were isolated in buffer containing DAPI and examined by fluorescence microscopy. In post-meiotic wild-type embryos, only the first polar body was DAPI labeled because it resides outside the permeability barrier of the *C. elegans* eggshell (Fig. 1B). Eggshell defects disrupt the permeability barrier, allowing DAPI labeling of zygotic chromatin. The zygotic chromatin of *sep-1(ax110* and *ax521)* embryos was accessible to DAPI, indicating eggshell defects (Fig. 1C; Table 2, lines 1–3).

To further assay the eggshell phenotype, we quantified the number and rate of CG exocytic events during anaphase I using an assay in which the incorporation of FM2-10 dye into the embryo plasma membrane is monitored at the sites of CG fusion (Bembenek et al., 2007). Both the new *sep-1* mutants showed a significant decrease in the total number and overall rate of CGE events (Fig. 3A,B,E,G) and had an increase in the time interval between the first and last CGE event (Fig. 3C; supplementary material Movies 2–4) when compared with wild-type embryos. Interestingly, although all the *sep-1(ax110)* embryos failed to extrude polar bodies, none ($n$=0/7) of them displayed nondisjunction during the first meiotic division (Fig. 2S,T). Therefore, we have identified two novel separation-of-function alleles of *sep-1* that are capable of promoting meiotic chromosome segregation, but fail to promote CGE.

### Characterization of SEP-1 localization in mutants

The SEP-1 protein has a dynamic localization pattern during meiosis I (Bembenek et al., 2007). As the maturing oocyte enters M phase, shortly before fertilization, SEP-1 localizes to cortical filaments (Bembenek et al., 2007). After fertilization, SEP-1 was found to localize to both the meiotic spindle and the CGs (Fig. 4A,B; Fig. 5). In mitotic embryos, SEP-1 localized to the spindle matrix during metaphase (Fig. 4C,D). We characterized the localization of the mutant SEP-1 proteins and detected several aberrations (Figs 4, 5). Previously, we found that SEP-1 in *sep-1(e2406ts)* embryos still localized to the anaphase I meiotic spindle, but not to CGs (Bembenek et al., 2007). The SEP-1 protein in *sep-1(ax110)* animals did not localize to any of these subcellular locations (Fig. 4I-L; Fig. 5). The SEP-1 protein in *sep-1(ax521)* animals still localized to cortical filaments in oocytes and the spindle matrix in meiotic embryos (Fig. 4E; Fig. 5), but was not observed on CGs during anaphase I (Fig. 4F; Fig. 5). It was also present on the spindle matrix in polyploid embryos cycling through mitosis (Fig. 4G,H). Western blot analysis revealed that the SEP-1 protein was produced in these mutants (supplementary material Fig. S1). Additionally, the distal germlines in all mutants contained abundant cytoplasmic SEP-1 that could be reduced upon *sep-1* RNAi feeding (data not shown).

### Characterization of *pph-5*-mediated suppression of *sep-1* lethality

We used the temperature-sensitive *sep-1(e2406ts)* allele to perform an EMS mutagenesis screen for secondary suppressor mutations at the non-permissive temperature of 20℃. Although most studies have shifted *sep-1(e2406ts)* animals to 25℃ (Bembenek et al., 2010; Bembenek et al., 2007; Siomos et al., 2001), we used 20℃, the lowest temperature at which embryonic lethality is fully penetrant. Three independent suppressors were recovered from screening 100,802 haploid genomes. Suppressors *av101* and *av102* mapped to linkage groups (LG) V and LG III, respectively, whereas *av103* was identified as an intragenic

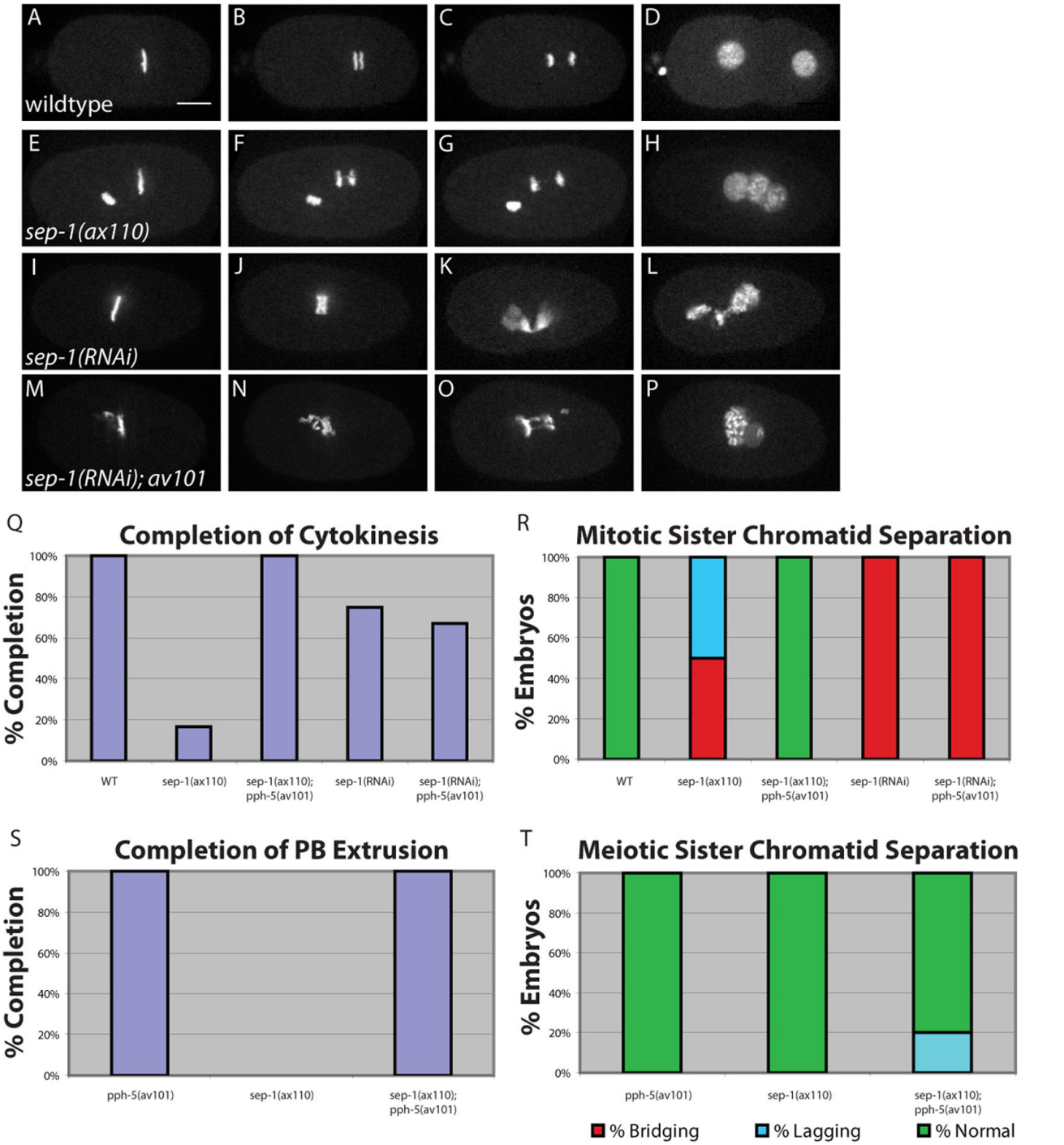


**Fig. 2. Novel *sep-1* mutants have weak nondisjunction but severe cytokinesis defects during mitosis.** Embryos of the indicated genotypes expressing GFP::H2B were imaged either in meiosis or mitosis (**A**–**P**) and scored for meiotic and mitotic chromosome segregation defects and completion of polar body extrusion during the meiotic divisions or cytokinesis during mitosis (**Q**–**T**). (A–D) A GFP::H2B-expressing wild-type embryo during the first mitotic division. Chromosome segregation and cytokinesis occurred normally in all embryos ($n$=5; S,T), resulting in a normal two-cell embryo (D). (E–H) *sep-1(ax110)* embryos showed weak chromosome nondisjunction during mitosis ($n$=6; F,G,S) but completed cytokinesis only 17% of the time (Q), resulting in polyploid one-cell embryos in the second mitotic division ($n$=6, H). *sep-1(ax110)* embryos did not have any nondisjunction during meiosis I despite failing polar body extrusion in every case we observed ($n$=7; S,T). (I–L) Partial depletion of *sep-1* by RNAi caused severe nondisjunction in all embryos ($n$=4; J,K,S) but only disrupted cytokinesis 25% of the time, similar to our previous results ($n$=4; L,T) (Bembenek et al., 2010). Stronger *sep-1(RNAi)* treatments completely prevented chromosome segregation (data not shown). (M–P) Loss of *pph-5* activity did not rescue the loss-of-function phenotypes of *sep-1(RNAi)* embryos ($n$=6; N,O,S) and cytokinesis failures were observed in 33% of the embryos, similar to the *sep-1* RNAi phenotype in wild-type embryos ($n$=6; P,T). In *sep-1(ax110);pph-5(av101)* embryos, no chromosome segregation defects ($n$=7; S) or cytokinesis failures were observed ($n$=6; T) during either meiosis or mitosis. Scale bar: 10 μm.

**Table 2. Novel *sep-1* mutants are permeable to DAPI**

| Strain | Embryos with DAPI-stained zygotic DNA | Embryos lacking PB extrusion |
|---|---|---|
| 1. *sep-1(+); GFP::H2B; pph-5(+)* | 0/34 | 0/34 |
| 2. *sep-1(ax110); GFP::H2B; pph-5(+)* | 13/24 | 21/24 |
| 3. *sep-1(ax521); GFP::H2B; pph-5(+)* | 13/23 | 22/23 |
| 4. *sep-1(+); GFP::H2B; pph-5(av101)* | 0/46 | 2/46 |
| 5. *sep-1(ax110); GFP::H2B; pph-5(av101)* | 0/20 | 2/20 |
| 6. *sep-1(ax521); GFP::H2B; pph-5(av101)* | 7/20 | 17/20 |

missense mutation (L556F) in *sep-1(e2406ts)* (Fig. 1A). The *av101* allele could suppress *sep-1(e2406ts)* at 20℃ (Table 1, compare lines 4 and 9), but not at 24℃ (Table 1, lines 5 and 11). Interestingly, *av101* could suppress the *sep-1(ax110)* mutation at all temperatures (Table 1, compare lines 2 and 7), but not *sep-1(ax521)* at any temperature (Table 1, lines 3 and 8, and data not shown). Curiously, *av101* suppressed *sep-1(e2406ts)* semi-dominantly, but behaved as a recessive suppressor with *sep-1(ax110)* (supplementary material Table S1). This semi-dominant suppression of *sep-1(e2406ts)* by *av101* suggests that the different *sep-1* alleles are sensitive to the dose of the protein mutated in *av101* animals. The allele *av102* failed to suppress either of these new *sep-1* alleles (data not shown). Neither *av101* nor *av102* was able to suppress *sep-1* RNAi or *sep-1(ok1749)* (data not shown). We also observed equivalent rates of chromosome nondisjunction and cytokinesis failures in wild-type and *av101* embryos treated with *sep-1* RNAi, suggesting that *av101* does not suppress *sep-1* RNAi at the cellular level (Fig. 2I–P,Q,R). Because these *sep-1* mutants have reduced chromosome segregation defects, it is probable that the new suppressors regulate the exocytic role of separase. The remainder of this report will focus on the characterization of the *av101* allele.

The *av101* allele was subjected to physical single nucleotide polymorphism (SNP) mapping, which refined its position to a 223 kb region predicted to contain 52 genes. A limited RNAi feeding screen identified Y39B6A.2 as a suppressor of *sep-1(ax110)* mutants; embryonic viability was restored to greater than 70% at 24℃ (Table 1, compare lines 2 and 17). Y39B6A.2 RNAi also suppressed *sep-1(e2406ts)* at 20℃ (Table 1, compare lines 4 and 10). Y39B6A.2 is the sole *C. elegans* ortholog of protein phosphatase 5, and led us to name it *pph-5*. Protein phosphatase 5 is widely conserved and is distinguished from other phosphatases by tetratricopeptide repeats (TPRs) at its N-terminus (Fig. 6A). Sequencing this gene from *av101* animals revealed a missense mutation that results in a Pro375Glu substitution in a highly conserved residue proximal to the active site (Swingle et al., 2004). An in-frame deletion allele of *pph-5*, *tm2979*, which removes 55 amino acids from the TPR array (Fig. 6A), also suppressed *sep-1(ax110* and *e2406ts)* (Table 1, lines 22 and 23). Interestingly, *pph-5(tm2979)* behaved similarly to *pph-5(av101)* in its ability to dominantly (but weakly) suppress *sep-1(e2406ts)*, but recessively suppress *sep-1(ax110)* (supplementary material Table S1). Wild-type animals bearing either *av101* or *tm2979* were healthy and fertile at all temperatures (Table 1, lines 6 and 20, and data not shown), even when exposed to further knockdown by *pph-5* RNAi (Table 1, compare lines 1 and 16 with lines 19 and 21). Because suppression by the *pph-5* alleles can be phenocopied by

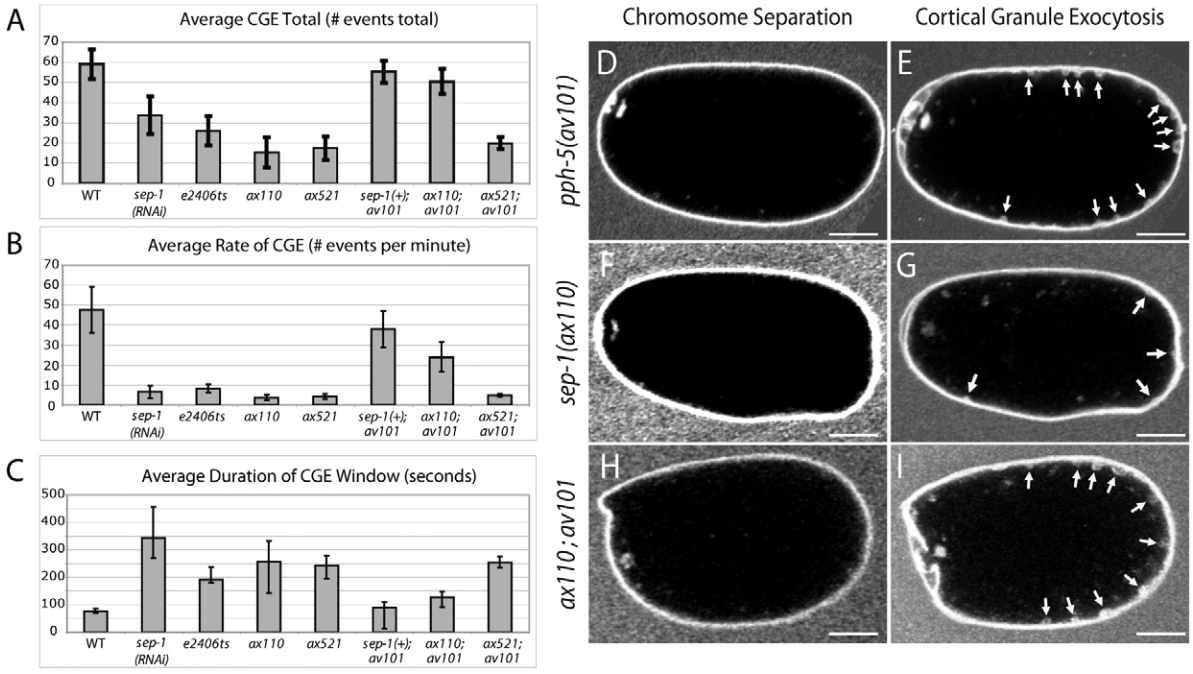


**Fig. 3. Quantification of the CGE defect of *sep-1* mutants.** (**A**) Average total number of CGE events per embryo. (**B**) Average rate of CGE events per embryo per minute. (**C**) Average duration of CGE window (the average time elapsed between the first and last CGE event, in seconds). At least six embryos were imaged for each genotype, and the bars indicate standard deviations. The data points for *sep-1(e2406ts)* and *sep-1(RNAi)* are from Bembenek et al. (Bembenek et al., 2007). (**D**–**I**) Chromosome separation occurred in both *av101* and *ax110* embryos (midplane images D and F), however, *ax110* had reduced numbers of CGE events (cortical time-projected images, E and G). CGE was restored in suppressed *sep-1(ax110); av101* (I). White arrows indicate sites of CGE. Scale bars: 10 μm.

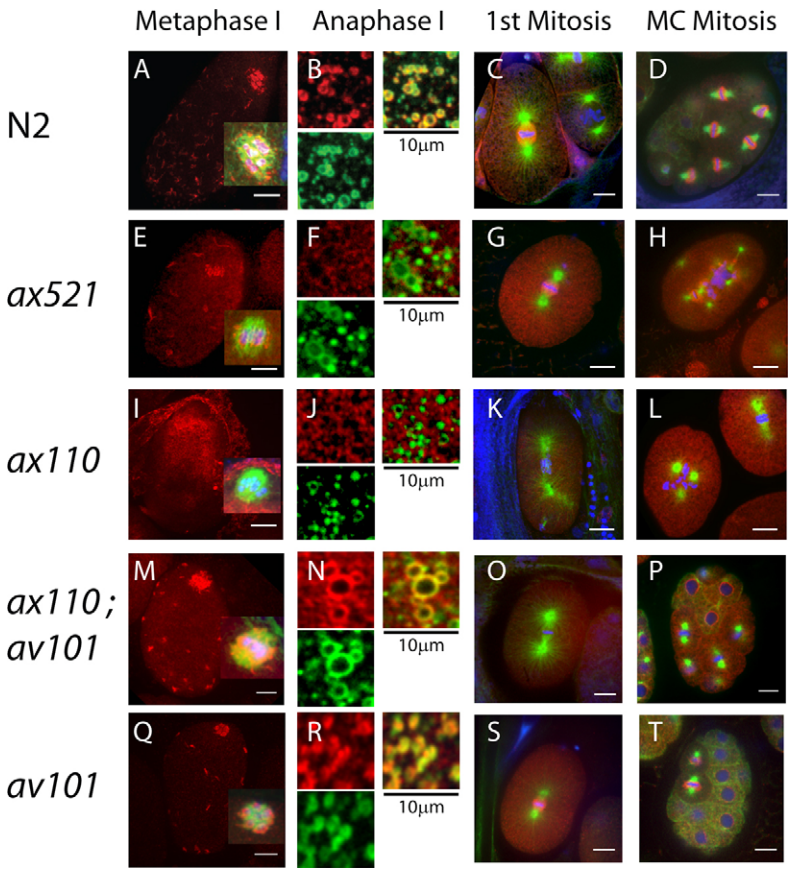


**Fig. 4. Subcellular localization of SEP-1 is defective in mutants.** Wild-type (N2), *sep-1(ax521)*, *sep-1(ax110)*, *sep-1(ax110); pph-5(av101)* and *pph-5(av101)* embryos were stained with anti-SEP-1 antibodies (Red; all panels), either anti-α-tubulin to label the spindle (Green; **A**,**C**,**D**,**E**,**G**,**H**,**I**,**K**,**L**,**M**,**O**,**P**,**Q**,**S**,**T**) or FITC::WGA to label cortical granules (green; **B**,**F**,**J**,**N**,**R**), and DAPI (blue; all panels). Images in the metaphase I column show SEP-1 localization (Red only), and the insets are 2× magnified images of the spindle shown in all three colors. The upper right images in the anaphase I column are merged images of anti-SEP-1 and the FITC::WGA. Colocalization appears yellow. Images in the first mitosis column are taken from embryos observed during the first mitotic metaphase, and the embryos depicted in the MC mitosis column are of multicellular (or multinucleate) embryos. Scale bars: 10 μm.

RNAi, we conclude that both alleles are reduction-of-function mutations. These alleles are not protein nulls as PPH-5 protein could be detected in animals bearing these mutations (Fig. 6B). The semi-dominant nature of *av101* suppression thus suggests that even a modest reduction in PPH-5 function is sufficient to suppress some *sep-1* mutant phenotypes. This hypothesis is supported by our observation that expression of PPH-5 protein was reduced but not completely abolished by RNAi feeding (supplementary material Fig. S2), even though this method suppressed both *sep-1(e2406ts* and *ax110)* mutants.

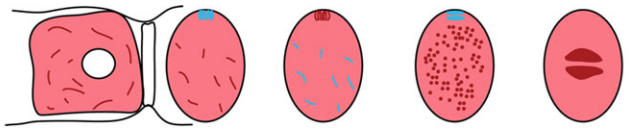

| Strain | -1 oocytes filaments | Metaphase I filaments | Meiotic Spindle Matrix | Anaphase I Cortical Granules | Mitotic Spindle Matrix |
|---|---|---|---|---|---|
| N2 | 14 / 32 | 32 / 34 | 48 / 52 | 3 / 6 | 63 / 63 |
| *sep-1(ax110)* | 0 / 17 | 0 / 6 | 0 /16 | 0 / 10 | 0 / 4 |
| *sep-1(ax521)* | 11 / 24 | 6 / 8 | 10 / 15 | 0 / 4 | 7 / 12 |
| *pph-5(av101)* | 22 / 35 | 8 / 9 | 20 / 25 | 3 / 6 | 15 / 15 |
| *ax110; av101* | 13 / 31 | 14 / 17 | 17 / 21 | 3 / 3 * | 0 / 53 |

**Fig. 5. Quantification of SEP-1 localization.** The presence of SEP-1 at cortical filaments, the meiotic spindle, cortical granules, and the mitotic spindle matrix was scored in each strain and the embryonic cell cycle stage was determined independently by inspecting the chromosome configuration with DAPI staining. The number of positively stained cells and the total number of cells examined for a particular cell cycle stage are shown. *The cortical granules of *sep-1(ax110)*; *pph-5(av101)* were labeled with SEP-1 antibodies, however, the overall intensity was reduced compared with wild-type embryos.

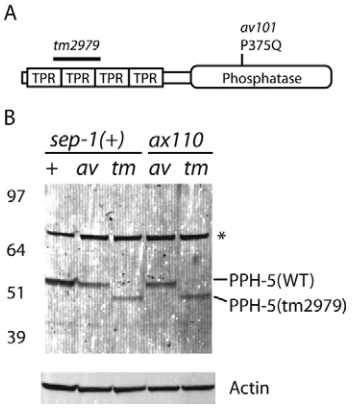


**Fig. 6. Schematic of the PPH-5 protein and PPH-5 expression data.** (**A**) A schematic representation of the *C. elegans* PPH-5 protein illustrates the arrangement of four tandem TPR domains and the PP2A-like phosphatase domain. The amino acid substitution caused by *av101* and the 55 amino acids removed by the *tm2979* deletion are indicated. (**B**) Mutant PPH-5 proteins were expressed. An immunoblot showing PPH-5 expression in *sep-1(+)* and *sep-1(ax110)* animals bearing the *pph-5(av101)* (*av*) or *pph-5(tm2979)* (*tm*) suppressor mutations. Each lane was loaded with protein equivalent to 50 gravid hermaphrodites. Actin was used as a loading control, and the asterisk indicates a non-specific cross-reactive band. Full-length and internally deleted PPH-5 proteins are expected to migrate at 56 and 50 kDa, respectively.

### CGE and SEP-1 localization defects are suppressed by *pph-5* mutations

We next investigated whether PPH-5 restores the membrane trafficking functions of the separase mutants. With regard to the DAPI permeability and CGE quantification assays, *sep-1(ax110); pph-5(av101)* embryos were indistinguishable from wild type, demonstrating that eggshell formation and CGE were no longer defective (Fig. 3; Table 2). In addition, *sep-1(ax110); pph-5(av101)* embryos were fully rescued from chromosome nondisjunction defects and cytokinesis failures during mitosis (Fig. 2Q,R). Polar body extrusion was also fully rescued (Fig. 2S). Disruption of *pph-5* had no effect on the eggshell and CGE defects observed in *sep-1(ax521)* mutant embryos; such double mutant embryos were still permeable to DAPI and failed to undergo CGE (data not shown).

Next we determined whether PPH-5 affected the localization of separase. Indeed, in *sep-1(ax110); pph-5(av101)* embryos, the localization of SEP-1 to the meiotic spindle and cortical filaments was restored (Fig. 4M). SEP-1 was also detected at the CGs during the first meiotic anaphase although at a reduced intensity compared with that in wild-type embryos (Fig. 4N; Fig. 5). We observed similar restoration of SEP-1 localization patterns when *sep-1(ax110)* was suppressed by *pph-5(tm2979)* or *pph-5(RNAi)* (data not shown). The subcellular localization of mutant SEP-1 in *sep-1(ax521)* embryos was not affected by *pph-5(av101)* (Fig. 5, data not shown). Surprisingly, although the *sep-1(ax110)*; *pph-5(av101)* embryos appeared to develop normally, SEP-1 localization to the mitotic spindle matrix was never observed (Fig. 4O,P; Fig. 5) but instead appeared cytoplasmic. The localization of wild-type SEP-1 was not affected in *pph-5(av101)* embryos (Fig. 4Q–T; Fig. 5). These data reveal that PPH-5 suppresses separase mutations by restoring its function during vesicle trafficking and not by a bypass mechanism. This is consistent with the fact that these *sep-1* alleles preferentially affected vesicle functions of separase more than chromosome segregation functions. This observation might account for the ability of *pph-5* mutations to suppress the hypomorphic *sep-1* alleles but not strict loss of function of *sep-1*. Therefore, PPH-5 is a negative regulator of the exocytic function of separase, influencing the localization of separase to vesicles at the appropriate times during cell division.

### PPH-5 expression and localization in the *C. elegans* germline

To determine the subcellular localization of PPH-5 in *C. elegans* embryos, a GFP::PPH-5 translational fusion was expressed using the germline-restricted *pie-1* promoter and 3′UTR sequences (Cheeseman and Desai, 2005; Reese et al., 2000) (see supplementary material Fig. S3A for schematic of the transgene). GFP::PPH-5 was cytoplasmic during interphase and became enriched at the spindle matrix in mitosis, similar to what is observed with GFP::SEP-1 and SEP-1 antibody staining (compare Fig. 7B,C with Fig. 4C,D) (Bembenek et al., 2007). The GFP::PPH-5 protein dispersed from the spindle during anaphase (supplementary material Movie 5). Attempts to confirm this pattern with various anti-PPH-5 staining protocols were unsuccessful, despite raising antibodies to many epitopes. Therefore, PPH-5 localizes to similar subcellular locations as separase during cell division, where it functions to regulate separase activity.

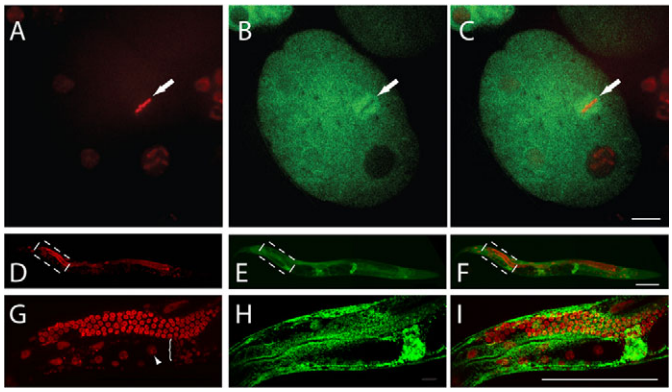


**Fig. 7. Expression and localization pattern of *pph-5* reporters.** (**A**–**C**) A four-cell embryo expressing *itIs37[pie-1p::mCherry::H2B::pie-1e]* (A), *avIs74[pie-1p::GFP(LAP)::PPH-5::pie-1e]* (B), and the merged image (C). GFP::PPH-5 localized to the spindle matrix in mitotic metaphase cells. The white arrows in A–C indicate the metaphase plate. Scale bar in C: 10 µm. (**D**–**I**) *pph-5* regulatory sequences were sufficient to drive expression of a mCherry::histone reporter in all somatic and germline tissues (D,G). A somatically expressed GFP reporter (*avIs112[manf-1p::GFP::manf-1::manf-1e]*) is shown in E and H, with merged images in F and I. The white dashed boxes in D–F are enlarged in G–I, respectively. The white arrowhead in G indicates the –1 oocyte, and the bracket denotes the spermatheca, which contains mCherry-positive spermatocytes. Scale bars in F and I: 100 µm.

To determine whether *pph-5* promoter sequences could also drive expression in the germline, we fused them to mCherry::histone H2B (supplementary material Fig. S3B). A line was generated and revealed robust levels of nuclear-localized mCherry signal in all cells at all developmental stages (Fig. 7D–I, and data not shown). This experiment suggests that the *pph-5* regulatory sequences can drive expression throughout development in somatic tissues and the entire germline.

### Depletion of PPH-5 in the germline is responsible for suppression

Because *pph-5* regulatory elements can drive expression in both the soma and germline, we investigated which tissue was relevant to the mechanism of *sep-1* suppression. We combined *sep-1(ax110)* with null alleles of *rrf-1* and *ppw-1*, which are defective for RNAi in somatic and germline tissues, respectively (Sijen et al., 2001; Tijsterman et al., 2002). Following feeding with *pph-5(RNAi)* bacteria, *sep-1(ax110) rrf-1(pk1417)* double mutants produced a viable brood at 24℃ (Table 3, lines 2, 4 and 6). Conversely, the *pph-5(RNAi)* feeding did not suppress the *sep-1(ax110) ppw-1(pk1425)* double mutant, suggesting that suppression requires functional germline RNAi (Table 3, lines 9, 13 and 17). This failure to suppress was not attributable to some novel interaction between *sep-1* and *ppw-1* because genetic suppression was still possible using *pph-5(tm2979)* (Table 3, compare lines 17 and 18). We conclude that suppression of *sep-1* embryonic lethality is mediated by interfering with the function of germline-derived PPH-5 protein.

## Discussion

### Characterization of two novel *sep-1* alleles with OID phenotypes

We have characterized two new alleles of the *sep-1* gene in *C. elegans*. Both *sep-1(ax110)* and *sep-1(ax521)* are recessive non-

**Table 3. Suppression of *sep-1* by *pph-5* RNAi is *ppw-1* dependent**

| Strain | RNAi | Total embryos | % Hatching |
|---|---|---|---|
| *1. sep-1(+) dpy-14(e188) rrf-1(pk1417)* | None | 486 | 95.3 |
| *2. sep-1(ax110) dpy-14(e188) rrf-1(pk1417)* | None | 661 | 0.0 |
| *3. sep-1(+) dpy-14(e188) rrf-1(pk1417)* | *smd-1* | 197 | 93.9 |
| *4. sep-1(ax110) dpy-14(e188) rrf-1(pk1417)* | *smd-1* | 657 | 0.0 |
| *5. sep-1(+) dpy-14(e188) rrf-1(pk1417)* | *pph-5* | 162 | 98.1 |
| *6. sep-1(ax110) dpy-14(e188) rrf-1(pk1417)* | *pph-5* | 490 | 57.6 |
| *7. sep-1(+) ppw-1(pk1425) dpy-5(e61)* | None | 619 | 98.4 |
| *8. sep-1(ax110) ppw-1(+) dpy-5(e61)* | None | 742 | 0.0 |
| *9. sep-1(ax110) ppw-1(pk1425) dpy-5(e61)* | None | 472 | 0.0 |
| *10. sep-1(ax110) ppw-1(pk1425) dpy-5(e61); pph-5(tm2979)* | None | 630 | 87.6 |
| *11. sep-1(+) ppw-1(pk1425) dpy-5(e61)* | *smd-1* | 524 | 95.4 |
| *12. sep-1(ax110) ppw-1(+) dpy-5(e61)* | *smd-1* | 646 | 0.0 |
| *13. sep-1(ax110) ppw-1(pk1425) dpy-5(e61)* | *smd-1* | 196 | 0.0 |
| *14. sep-1(ax110) ppw-1(pk1425) dpy-5(e61); pph-5(tm2979)* | *smd-1* | 520 | 95.8 |
| *15. sep-1(+) ppw-1(pk1425) dpy-5(e61)* | *pph-5* | 555 | 96.4 |
| *16. sep-1(ax110) ppw-1(+) dpy-5(e61)* | *pph-5* | 364 | 61.5 |
| *17. sep-1(ax110) ppw-1(pk1425) dpy-5(e61)* | *pph-5* | 384 | 0.8 |
| *18. sep-1(ax110) ppw-1(pk1425) dpy-5(e61); pph-5(tm2979)* | *pph-5* | 469 | 94.7 |

Embryonic survival assays of various mutant combinations were performed at 24℃ to test the dependence of *pph-5(RNAi)* suppression on tissue-specific RNAi machinery. Lines 1–6 show that functional somatic RNAi is not required for *pph-5* RNAi to suppress *sep-1(ax110)*, whereas lines 7–18 indicate that *ppw-1*-dependent germline RNAi is required for suppression. The *smd-1* gene was used as a negative control (lines 3, 4, 11–14). The RNAi-defective mutants *rrf-1(pk1417)* and *ppw-1(pk1425)* used in this assay were linked to *dpy-14(e188)* and *dpy-5(e61),* respectively. These morphological markers had no effect on the embryonic lethality of *sep-1(ax110)* or its suppression by depletion of *pph-5* (lines 8, 12, 16, and data not shown).

conditional alleles and embryos bearing these alleles have defects similar to those exhibited by *sep-1(e2406ts)* embryos. Importantly, all three alleles cause limited defects in sister chromatid separation. Instead, these alleles disrupt the function of separase during vesicle trafficking. The amino acid substitutions encoded by *e2406ts* and *ax521* lie well outside the peptidase domain. The *ax110* allele harbors a mutation in a non-conserved residue that resides just within this domain. Thus it is probable that these alleles do not inactivate the catalytic activity required for cohesin cleavage. This contrasts with mutant alleles of separase in other organisms in which they disrupt the cohesin cleavage activity of separase (López-Avilés and Uhlmann, 2010). Therefore, these alleles provide a unique opportunity to examine the function of separase in vesicle trafficking.

Although it is well established that the cleavage of cohesin is a conserved function of separase, there is mounting evidence that separase has many roles during cell division, including some that do not require its protease activity (Gorr et al., 2006; Kudo et al., 2006; López-Avilés and Uhlmann, 2010). Gorr et al. have shown that specific anti-separase antibodies, which do not interfere with the cleavage of cohesin but prevent the interaction between separase and Cdk1, inhibit the extrusion of polar bodies when injected into *Xenopus* oocytes (Gorr et al., 2006). Similar results were reported using separase-null mouse oocytes, which have a polar body extrusion defect that can be rescued by injection of mRNA encoding catalytically inactive separase (Kudo et al., 2006). Whether these data reflect a role for separase in CGE in vertebrate oocytes remains to be determined.

High resolution electron micrographs have revealed that *sep-1(e2406ts)* embryos fail to form the chitin and lipid-rich inner layers of the eggshell (Bembenek et al., 2007; Benenati et al., 2009). The reduced level of CGE observed in *sep-1*-deficient animals is a probable cause for these defects in the eggshell, because the CGs contain the raw materials required for assembly of the mature eggshell (Bembenek et al., 2007; Sato et al., 2006). Consistent with this observation, we find that all the SEP-1 mutant proteins fail to properly localize to CGs during anaphase (Fig. 3). Hence, we conclude that these alleles are hypomorphic for a subset of *sep-1* functions, including vesicle exocytosis. However far removed the role of separase is in CGE from its canonical role in cohesin cleavage, it is likely that it still falls under the regulation of securin and the APC/C, because loss of expression of these genes also disrupts the eggshell and interferes with CG trafficking (Bembenek et al., 2007; Golden et al., 2000; Shakes et al., 2003; Wallenfang and Seydoux, 2000). It will be interesting to determine whether a catalytically inactive version of SEP-1 can rescue these particular phenotypes in *C. elegans* embryos, as has been shown for the polar body extrusion defects in separase-deficient mouse oocytes (Kudo et al., 2006).

### Aberrant SEP-1 localization in mutant embryos

Separase has a dynamic subcellular localization pattern in early *C. elegans* embryos (Bembenek et al., 2007). The novel *sep-1* mutants can be distinguished from one another by the subcellular localization of their respective mutant proteins. *sep-1(ax521)* mutants had a SEP-1 localization defect that was specific to CGs. A more general defect was observed in *sep-1(ax110)* animals where SEP-1 failed to localize to the cortical structures, the spindle matrix or the CGs. Therefore, these mutant proteins probably disrupt the function of separase by disrupting its subcellular localization. We speculate that the spindle localization of the SEP-1 protein might reflect its roles in regulation of the anaphase spindle or membrane trafficking dynamics rather than cohesin cleavage. This conclusion is supported by the finding that separase can directly bind DNA in vitro, facilitating its access to and cleavage of cohesin (Sun et al., 2009), which is probably unperturbed with these novel mutant proteins.

### Mutations in the *pph-5* gene suppress *sep-1* embryonic lethality

Using a genetic suppression screen of the conditional *sep-1(e2406ts)* allele, two extragenic mutations were isolated that

restored fertility and viability at 20℃. Performing the screen at 20℃ was instrumental in recovering these suppressor mutations; neither allele suppressed *sep-1(e2406ts)* at 24℃. One of these suppressors is an allele of *pph-5*; PPH-5 is a conserved protein involved in several cell signaling pathways (Hinds and Sánchez, 2008). The in-frame deletion allele *pph-5(tm2979)* suppresses *sep-1(e2406ts)* and *sep-1(ax110)* to the same extent as *pph-5(av101)*. *pph-5* RNAi also suppresses *sep-1(e2406ts)* and *sep-1(ax110)*, suggesting that a general reduction in *pph-5* activity is the causal factor leading to the restoration of viability of *sep-1* embryos. We therefore conclude that *pph-5(av101)* and *pph-5(tm2979)* are reduction-of-function mutations.

Although the *sep-1(e2406ts)* mutant was used in our suppressor screen, only *sep-1(ax110)* is fully suppressed (at all temperatures) by *pph-5* mutations or RNAi. The *sep-1(ax521)* allele is not suppressed by loss of *pph-5*, and *sep-1(e2406ts)* is only suppressed up to 20℃. It remains to be determined whether this suppression profile reflects the strength of each of the *sep-1* alleles, the pleiotropic nature of each or the structural and/or conformational alteration caused by each of these missense mutations. Interestingly, the two mutations that are not fully suppressed are both located in the large N-terminal domain of separase, well outside the catalytic domain.

Because the synthesis of a mature eggshell is essential to the survival of the embryo (Rappleye et al., 1999), it is not surprising that our screen isolated a secondary mutation that restored CGE and eggshell function. Although the function of SEP-1 at its various localities is not understood, it is important to note that suppression restored the localization of separase to vesicles and the efficient fusion of CGs with the plasma membrane in *sep-1(ax110)* embryos. This finding suggests that the mechanism of suppression involves restoring the function of a defective SEP-1 protein as opposed to bypassing it altogether, such as by stimulating exocytosis through another pathway. This would also explain why the suppression seems to be specific to certain *sep-1* alleles, and does not suppress the effect of *sep-1(ax521)* or *sep-1(RNAi)* where separase cannot be restored to vesicles. It will be interesting to determine the mechanism underlying the recruitment of separase to vesicles and how PPH-5 is involved.

Despite our observations that modulating the level of *pph-5* activity can have dramatic effects on the survival of two distinct separase mutants, this gene appears to be non-essential. Although the *pph-5* alleles behave as hypomorphic mutations, their catalytic domains are intact (Fig. 6). Therefore the question of whether *pph-5* is essential for embryonic development remains unanswered until a true null allele becomes available. Nonetheless, the two *pph-5* alleles behave as 'silent' suppressors of *sep-1* mutants, and thus highlight how beneficial genetic screens are for identifying novel factors that regulate the separase pathway.

Interestingly, mice homozygous for a deletion in the murine protein phosphatase 5 (Ppp5) gene are viable and fertile (Yong et al., 2007). Mouse embryonic fibroblasts from such embryos, however, exhibit defects in the DNA damage checkpoint arrest in response to ionizing radiation. To date, no mutant phenotypes have been reported for the *Drosophila* or *S. cerevisiae* protein phosphatase 5 orthologs (Chen et al., 1994).

### Phosphatase regulation of the separase pathway

Because *pph-5* encodes a phosphatase, we hypothesize that the reduction of *pph-5* activity causes a net increase in the phosphorylated subpopulation of one or more target proteins. This persistent phosphorylation might affect enzymatic activity, protein–protein interactions, or subcellular localizations of proteins in the SEP-1 pathway. There are examples of phosphorylation playing such roles for many components of the separase pathway including cohesin, Cdc27 and separase itself (Huang et al., 2007; Huang et al., 2009; Kudo et al., 2009). Our finding that the reduced activity of *pph-5* restores CG localization of SEP-1 in *sep-1(ax110)* embryos suggests that the subcellular localization of SEP-1 to CGs might be regulated by phosphorylation. This regulation could be direct and phosphorylation of SEP-1 (or an associated protein) could be essential for the movement of SEP-1 to CGs. Alternatively, suppression could involve a more indirect pathway whereby PPH-5 regulates the activity of an upstream regulator of separase. Ultimately, elucidating the mechanisms employed by PPH-5 to regulate the localization of separase to vesicles and its exocytic activity will be a fascinating subject of future studies.

In yeast, the phosphatase PP2A acts as a regulator of the separase pathway (Clift et al., 2009; Riedel et al., 2006). Rec8 only serves as a separase substrate when it is phosphorylated during meiosis (Riedel et al., 2006). When PP2A is targeted to centromeres by shugoshin, it removes phosphates from the neighboring cohesin complexes thereby reducing their suitability as separase substrates and ultimately leads to the protection of centromeric cohesion during meiosis I (Riedel et al., 2006). Perhaps PPH-5 in *C. elegans* plays an analogous role and removes phosphates from vesicle proteins to reduce their affinity as SEP-1 interacting proteins/substrates. In *sep-1; pph-5* suppressed mutants, these phospho-epitopes might persist, allowing a 'compromised' separase more time to recognize and cleave its phosphorylated vesicle substrates.

In mammalian systems, separase is the target of an inhibitory phosphorylation that occurs on serine 1126 (Stemmann et al., 2001), which is in the unstructured region adjacent to the peptidase domain. In vitro experiments have shown that Cdc2–cyclinB and MAPK can phosphorylate S1126 of purified separase (Stemmann et al., 2001). Phosphorylation of S1126 is a prerequisite for separase to bind cyclinB directly, an interaction that mutually inhibits both the protease activity of Sep1 and the kinase activity of Cdk1–cyclinB (Gorr et al., 2005). Although it is unknown whether these regulatory mechanisms are conserved in *C. elegans*, or whether CDK-1 interactions affect the localization of SEP-1, our data does support the view that the exocytic functions of separase is regulated by an interplay between kinases and phosphatases. Whatever the mechanism, our findings strongly suggest that the exocytic function of separase in *C. elegans* is influenced by the phosphatase PPH-5; identifying its substrates is key to unraveling the novel regulatory mechanism of separase function in membrane trafficking.

## Materials and Methods

### Strains and alleles

Wild-type *C. elegans* was the Bristol strain N2. All strains were cultured using standard techniques (Brenner, 1974). Temperature-sensitive strains were maintained at 15℃; all other strains were maintained at 20℃.

Other strains used were: AG185: *pph-5(av101);* AG186: *pph-5(tm2979);* AG187: *dpy-21(e428) rol-9(sc148);* AG188: *sep-1(e2406ts); dpy-21(e428) pph-5(av101) rol-9(sc148);* AG189: *sep-1(ax110); dpy-21(e428) pph-5(av101) rol-9(sc148);* AG190: *sep-1(ax110) dpy-5(e61)/hT2[qIs48];* AG191: *sep-1(ax110) ppw-1(pk1425) dpy-5(e61)/hT2[qIs48];* AG192: *ppw-1(pk1425) dpy-5(e61);* AG193: *sep-1(ax110) dpy-5(e61); pph-5(tm2979);* AG194: *unc-119(ed3); ltIs37[pAA64: pie-1/mCherry::his-58 + unc-119 (+)]; avIs74[pCR305 (pie-1p:LAP::pph-5::pie-1e + unc-119(+)];* AG197: *unc-119(ed3); avIs90[pCR450 (pph-5p::mCherry::H2B::pph-5e + unc-119(+)];* AG198: *sep-1(ax110); unc-119(ed3) ruIs32[pie-1p::GFP::H2B + unc-*

*119(+)]; pph-5(av101);* AG199: *sep-1(ax110)* (9 × outcross to CB4856); BS3608: *dpy-14(e188) rrf-1(pk1417)I;* CB4856 (Hawaiian); CB61: *dpy-5(e61)I;* CB188: *dpy-14(e188)I;* CB428: *dpy-21(e428)V;* NL3511: *ppw-1(pk1425)I;* OD57: *unc-119(ed3); ltIs37[pAA64: pie-1p::mCherry::his-58 + unc-119 (+)]; itIs25 [pAZ132: pie-1p::GFP::tba-2 + unc-119(+)];* VC1284: *sep-1(ok1749)/hT2[qIs48];* WH408: *sep-1(e2406ts)/hT2[qIs48];* WH410: *sep-1(ax110)/hT2[qIs48];* WH409: *sep-1(ax521)/ hT2[qIs48];* WH468: *sep-1(e2406ts)/hT2[qIs48]; unc-119(ed3) ruIs32[pie-1p::GFP::H2B + unc-119(+)]/ hT2[qIs48];* WH470: *sep-1(ax110)/hT2[qIs48]; unc-119(ed3) ruIs32[pie-1p::GFP::H2B + unc-119(+)]/ hT2[qIs48];* WH469: *sep-1(ax521)/hT2[qIs48]; unc-119(ed3) ruIs32[pie-1p::GFP::H2B + unc-119(+)]/ hT2[qIs48].*

### Quantification of the Emb phenotype

L4 animals shifted to the restrictive temperature for 12–24 hours were moved daily to new plates; hatched and unhatched progeny were counted 24 hours later.

### DAPI permeability assay

L4 homozygous *sep-1* mutants were shifted to 24℃ for 12–24 hours. Embryos isolated in egg buffer (118 mM NaCl, 48 mM KCl, 2 mM $CaCl_2{\cdot}2H_2O$, 2 mM $MgCl_2{\cdot}6H_2O$, 25 mM Hepes pH 7.3) containing DAPI (5 μg/ml) were mounted on an agar pad, and examined by UV epifluorescence.

### Quantification of cortical granule exocytosis

CGE was quantified according to a protocol previously published (Bembenek et al., 2007).

### Time-lapse imaging of embryos

The time-lapse images of *avIs74; itIs37* embryos were taken on a Nikon Eclipse TE2000U microscope equipped with a 603 1.4 NA Plan Apo objective along with a Spectral Applied Research LMM5 laser merge module, a Yokogawa CSU10 spinning disk unit, and a Hamamatsu C9100-13 EM-CCD camera. Image processing and AVI production were carried out using ImageJ 1.42q software (Abramoff et al., 2004).

### Antibody staining and confocal microscopy

Embryos were isolated in Edgar buffer (60 mM NaCl, 32 mM KCl, 3 mM $Na_2HPO_4$, 2 mM $MgCl_2$, 2 mM $CaCl_2$, 5 mM Hepes, pH 7.2, 0.2% glucose) plus 4 mM levamisole (Boyd et al., 1996), overlaid with a coverslip, and freeze-cracked. Specimens were fixed in methanol at 22℃ for 5 minutes, and then rehydrated in TBS with 0.1% Tween 20 (TBST) for 15 minutes. Antibodies were diluted in TBST with 1% goat serum. Confocal microscopic images were acquired with a Nikon Eclipse E800 microscope equipped with a PerkinElmer Ultra*VIEW* spinning disk unit and an Hamamatsu C9100-12 EM-CCD camera using Openlab software (Improvision, Inc.). Image processing was completed using ImageJ and Adobe Photoshop software.

### Sequencing new *sep-1* alleles

Sequencing was performed by Seqwright (Houston, TX) on a PCR-amplified 9 kb region containing the entire *sep-1* gene. The alleles *e2406ts, ax110*, and *ax521* create novel restriction sites, *Acc*I, *Sac*II and *Rsa*I, respectively, which were used for PCR-based genotyping. The oligonucleotides used for sequencing and genotyping are compiled in supplementary material Table S2.

### Genetic screen for suppression of *sep-1(e2406ts)*

L4 *sep-1(e2406ts)* homozygotes were grown at 15℃ and mutagenized with 50 mM ethyl methanesulfonate (EMS). After two generations at 15℃, plates were shifted to 20℃, the minimum temperature at which embryonic lethality is fully penetrant. Suppressed lines were isolated, retested for viability at 20° and 24℃, and then backcrossed to *sep-1(e2406ts)*. Assignment to linkage groups was done using standard single nucleotide polymorphism (SNP) mapping (Davis et al., 2005; Wicks et al., 2001), followed by three factor mapping (see below).

### Genetic mapping of *pph-5(av101)*

*pph-5(av101)* was mapped to the right arm of LG V by SNP mapping. SNP mapping was carried out using the *sep-1(ax110)* allele, which was back-crossed into the Hawaiian strain CB4856. Three factor mapping was carried out with *sep-1(ax110)*; *dpy-21(e428) pph-5(av101) rol-9(sc148)* hermaphrodites. Molecular genotyping was performed using single animal PCR and the standard SNP-snip protocol (Wicks et al., 2001). DNA from *pph-5(av101)* animals was sequenced by Seqwright or MWG (Gaithersburg, MD).

### Isolation of the *pph-5(tm2979)* deletion allele

The *pph-5(tm2979)* allele was obtained from Shohei Mitano (Tokyo Women's Medical University, Japan), backcrossed to N2 nine times, and the 165 bp deletion was confirmed by PCR.

### RNAi feeding

MYOB plates (Church et al., 1995) augmented with carbenicillin and isopropyl-β-D-thiogalactopyranoside were seeded with HT115(DE3) bacteria harboring the L4440-based RNAi feeding constructs. Embryonic hatching was determined as stated above, except that broods hatching in the first 24 hours were not included in our analysis. RNAi constructs were obtained from the Ahringer library (Kamath and Ahringer, 2003) (Geneservice, Cambridge, UK) or were made from genomic DNA Gateway-cloned into the RNAi feeding vector pCR88.

### Microparticle bombardment

Microparticle bombardment was performed according to standard protocols (Praitis et al., 2001) except that animals were grown in liquid culture before transformation.

### PPH-5 detection by western blot

Asynchronous animals were washed and resuspended in 1× LDS buffer (Invitrogen, Carlsbad, CA) with β-mercaptoethanol and incubated at 95℃ for 10 minutes. Lysates were separated on 4–12% Bis-Tris NuPage gels with MOPS buffer (Invitrogen) and transferred to polyvinylidene fluoride (PDVF) membrane (Invitrogen). PPH-5 was detected using an affinity-purified rabbit antibody directed against the peptide sequence CAIEDSYDGPRLEDKITKEFV (amino acids 171–190; Covance, Inc.). This peptide was conjugated to keyhole limpet hemocyanin and was also used in the purification of these antisera. Actin was detected using the mouse monoclonal antibody C4 from Millipore (Billerica, MA). Secondary antibodies used were anti-rabbit 700 and anti-mouse 800 from Li-Cor (Lincoln, NE). All antibody incubations were done in the presence of 1× Li-Cor blocking buffer.

We acknowledge Mike Boxem (Harvard Medical School) for pDEST-MB16, Shohei Mitani (Tokyo Women's Medical University School of Medicine) for generating the *pph-5(tm2979)* allele and the *C. elegans* Gene Knockout Consortium (Oklahoma Medical Research Foundation) for generating the *sep-1(ok1749)* allele. Some strains were provided by the *Caenorhabditis* Genetics Center, funded by the NIH National Center for Research Resources. We are grateful for the suggestions and comments from Kevin O'Connell, Kathryn Stein, and members of the Baltimore Worm Club. This research was supported by NIH grant 5R01GM062181 (J.M.S.) and the Intramural Research Program of the NIH, National Institute of Diabetes and Digestive and Kidney Diseases (A.G.). Deposited in PMC for release after 12 months.

Supplementary material available online at
http://jcs.biologists.org/lookup/suppl/doi:10.1242/jcs.073379/-/DC1

## References

**Abramoff, M., Magelhaes, P. and Ram, S.** (2004). Image processing with ImageJ. *Biophotonics Int.* **11**, 36-42.

**Agarwal, R. and Cohen-Fix, O.** (2002). Phosphorylation of the mitotic regulator Pds1/securin by Cdc28 is required for efficient nuclear localization of Esp1/separase. *Genes Dev.* **16**, 1371-1382.

**Alexandru, G., Uhlmann, F., Mechtler, K., Poupart, M. A. and Nasmyth, K.** (2001). Phosphorylation of the cohesin subunit Scc1 by Polo/Cdc5 kinase regulates sister chromatid separation in yeast. *Cell* **105**, 459-472.

**Bacac, M., Fusco, C., Planche, A., Santodomingo, J., Demaurex, N., Leemann-Zakaryan, R., Provero, P. and Stamenkovic, I.** (2011). Securin and separase modulate membrane traffic by affecting endosomal acidification. *Traffic* **12**, 615-626.

**Bard, F., Casano, L., Mallabiabarrena, A., Wallace, E., Saito, K., Kitayama, H., Guizzunti, G., Hu, Y., Wendler, F., Dasgupta, R. et al.** (2006). Functional genomics reveals genes involved in protein secretion and Golgi organization. *Nature* **439**, 604-607.

**Bembenek, J., White, J. and Zheng, Y.** (2010). A role for separase in the regulation of RAB-11-positive vesicles at the cleavage furrow and midbody. *Curr. Biol.* **20**, 259-264.

**Bembenek, J. N., Richie, C. T., Squirrell, J. M., Campbell, J. M., Eliceiri, K. W., Poteryaev, D., Spang, A., Golden, A. and White, J. G.** (2007). Cortical granule exocytosis in *C. elegans* is regulated by cell cycle components including separase. *Development* **134**, 3837-3848.

**Benenati, G., Penkov, S., Muller-Reichert, T., Entchev, E. V. and Kurzchalia, T. V.** (2009). Two cytochrome P450s in *Caenorhabditis elegans* are essential for the organization of eggshell, correct execution of meiosis and the polarization of embryo. *Mech. Dev.* **126**, 382-393.

**Boyd, L., Guo, S., Levitan, D., Stinchcomb, D. T. and Kemphues, K. J.** (1996). PAR-2 is asymmetrically distributed and promotes association of P granules and PAR-1 with the cortex in *C. elegans* embryos. *Development* **122**, 3075-3084.

**Brenner, S.** (1974). The genetics of *Caenorhabditis elegans*. *Genetics* **77**, 71-94.

**Cheeseman, I. M. and Desai, A.** (2005). A combined approach for the localization and tandem affinity purification of protein complexes from metazoans. *Sci STKE* **2005**, pl1.

**Chen, M. X., McPartlin, A. E., Brown, L., Chen, Y. H., Barker, H. M. and Cohen, P. T.** (1994). A novel human protein serine/threonine phosphatase, which possesses four tetratricopeptide repeat motifs and localizes to the nucleus. *EMBO J.* **13**, 4278-4290.

**Church, D. L., Guan, K. L. and Lambie, E. J.** (1995). Three genes of the MAP kinase cascade, *mek-2*, *mpk-1/sur-1* and *let-60 ras*, are required for meiotic cell cycle progression in *Caenorhabditis elegans*. *Development* **121**, 2525-2535.

**Clift, D., Bizzari, F. and Marston, A. L.** (2009). Shugoshin prevents cohesin cleavage by PP2A(Cdc55)-dependent inhibition of separase. *Genes Dev.* **23**, 766-780.

**Davis, M. W., Hammarlund, M., Harrach, T., Hullett, P., Olsen, S. and Jorgensen, E. M.** (2005). Rapid single nucleotide polymorphism mapping in *C. elegans*. *BMC Genomics* **6**, 118.

**Golden, A., Sadler, P. L., Wallenfang, M. R., Schumacher, J. M., Hamill, D. R., Bates, G., Bowerman, B., Seydoux, G. and Shakes, D. C.** (2000). Metaphase to anaphase (mat) transition-defective mutants in *Caenorhabditis elegans*. *J. Cell Biol.* **151**, 1469-1482.

**Gorr, I. H., Boos, D. and Stemmann, O.** (2005). Mutual inhibition of separase and Cdk1 by two-step complex formation. *Mol. Cell* **19**, 135-141.

**Gorr, I. H., Reis, A., Boos, D., Wuhr, M., Madgwick, S., Jones, K. T. and Stemmann, O.** (2006). Essential CDK1-inhibitory role for separase during meiosis I in vertebrate oocytes. *Nat. Cell Biol.* **8**, 1035-1037.

**Hinds, T. D. and Sánchez, E. R.** (2008). Protein phosphatase 5. *Int. J. Biochem. Cell Biol.* **40**, 2358-2362.

**Huang, J. Y., Morley, G., Li, D. and Whitaker, M.** (2007). Cdk1 phosphorylation sites on Cdc27 are required for correct chromosomal localisation and APC/C function in syncytial *Drosophila* embryos. *J. Cell Sci.* **120**, 1990-1997.

**Huang, X., Andreu-Vieyra, C. V., Wang, M., Cooney, A. J., Matzuk, M. M. and Zhang, P.** (2009). Preimplantation mouse embryos depend on inhibitory phosphorylation of separase to prevent chromosome missegregation. *Mol. Cell. Biol.* **29**, 1498-1505.

**Johnston, W. L., Krizus, A. and Dennis, J. W.** (2010). Eggshell chitin and chitin-interacting proteins prevent polyspermy in *C. elegans*. *Curr. Biol.* **20**, 1932-1937.

**Kamath, R. S. and Ahringer, J.** (2003). Genome-wide RNAi screening in *Caenorhabditis elegans*. *Methods* **30**, 313-321.

**Kudo, N. R., Wassmann, K., Anger, M., Schuh, M., Wirth, K. G., Xu, H., Helmhart, W., Kudo, H., McKay, M., Maro, B. et al.** (2006). Resolution of chiasmata in oocytes requires separase-mediated proteolysis. *Cell* **126**, 135-146.

**Kudo, N. R., Anger, M., Peters, A. H., Stemmann, O., Theussl, H. C., Helmhart, W., Kudo, H., Heyting, C. and Nasmyth, K.** (2009). Role of cleavage by separase of the Rec8 kleisin subunit of cohesin during mammalian meiosis I. *J. Cell Sci.* **122**, 2686-2698.

**López-Avilés, S. and Uhlmann, F.** (2010). Cell cycle: the art of multi-tasking. *Curr. Biol.* **20**, R101-R103.

**Olson, S. K., Bishop, J. R., Yates, J. R., Oegema, K. and Esko, J. D.** (2006). Identification of novel chondroitin proteoglycans in *Caenorhabditis elegans*: embryonic cell division depends on CPG-1 and CPG-2. *J. Cell Biol.* **173**, 985-994.

**Praitis, V., Casey, E., Collar, D. and Austin, J.** (2001). Creation of low-copy integrated transgenic lines in *Caenorhabditis elegans*. *Genetics* **157**, 1217-1226.

**Rappleye, C. A., Paredez, A. R., Smith, C. W., McDonald, K. L. and Aroian, R. V.** (1999). The coronin-like protein POD-1 is required for anterior-posterior axis formation and cellular architecture in the nematode *Caenorhabditis elegans*. *Genes Dev.* **13**, 2838-2851.

**Reese, K. J., Dunn, M. A., Waddle, J. A. and Seydoux, G.** (2000). Asymmetric segregation of PIE-1 in *C. elegans* is mediated by two complementary mechanisms that act through separate PIE-1 protein domains. *Mol. Cell* **6**, 445-455.

**Riedel, C. G., Katis, V. L., Katou, Y., Mori, S., Itoh, T., Helmhart, W., Galova, M., Petronczki, M., Gregan, J., Cetin, B. et al.** (2006). Protein phosphatase 2A protects centromeric sister chromatid cohesion during meiosis I. *Nature* **441**, 53-61.

**Rogers, E., Bishop, J. D., Waddle, J. A., Schumacher, J. M. and Lin, R.** (2002). The aurora kinase AIR-2 functions in the release of chromosome cohesion in *Caenorhabditis elegans* meiosis. *J. Cell Biol.* **157**, 219-229.

**Sato, K., Sato, M., Audhya, A., Oegema, K., Schweinsberg, P. and Grant, B. D.** (2006). Dynamic regulation of caveolin-1 trafficking in the germ line and embryo of *Caenorhabditis elegans*. *Mol. Biol. Cell* **17**, 3085-3094.

**Sato, M., Grant, B. D., Harada, A. and Sato, K.** (2008). Rab11 is required for synchronous secretion of chondroitin proteoglycans after fertilization in *Caenorhabditis elegans*. *J. Cell Sci.* **121**, 3177-3186.

**Shakes, D. C., Sadler, P. L., Schumacher, J. M., Abdolrasulnia, M. and Golden, A.** (2003). Developmental defects observed in hypomorphic anaphase-promoting complex mutants are linked to cell cycle abnormalities. *Development* **130**, 1605-1620.

**Sijen, T., Fleenor, J., Simmer, F., Thijssen, K. L., Parrish, S., Timmons, L., Plasterk, R. H. and Fire, A.** (2001). On the role of RNA amplification in dsRNA-triggered gene silencing. *Cell* **107**, 465-476.

**Siomos, M. F., Badrinath, A., Pasierbek, P., Livingstone, D., White, J., Glotzer, M. and Nasmyth, K.** (2001). Separase is required for chromosome segregation during meiosis I in *Caenorhabditis elegans*. *Curr. Biol.* **11**, 1825-1835.

**Stemmann, O., Zou, H., Gerber, S. A., Gygi, S. P. and Kirschner, M. W.** (2001). Dual inhibition of sister chromatid separation at metaphase. *Cell* **107**, 715-726.

**Sun, Y., Kucej, M., Fan, H. Y., Yu, H., Sun, Q. Y. and Zou, H.** (2009). Separase is recruited to mitotic chromosomes to dissolve sister chromatid cohesion in a DNA-dependent manner. *Cell* **137**, 123-132.

**Suzuki, Y., Kagawa, N., Fujino, T., Sumiya, T., Andoh, T., Ishikawa, K., Kimura, R., Kemmochi, K., Ohta, T. and Tanaka, S.** (2005). A novel high-throughput (HTP) cloning strategy for site-directed designed chimeragenesis and mutation using the Gateway cloning system. *Nucleic Acids Res* **33**, e109.

**Swingle, M. R., Honkanen, R. E. and Ciszak, E. M.** (2004). Structural basis for the catalytic activity of human serine/threonine protein phosphatase-5. *J. Biol. Chem.* **279**, 33992-33999.

**Tijsterman, M., Okihara, K. L., Thijssen, K. and Plasterk, R. H.** (2002). PPW-1, a PAZ/PIWI protein required for efficient germline RNAi, is defective in a natural isolate of *C. elegans*. *Curr. Biol.* **12**, 1535-1540.

**Timmons, L., Court, D. L. and Fire, A.** (2001). Ingestion of bacterially expressed dsRNAs can produce specific and potent genetic interference in *Caenorhabditis elegans*. *Gene* **263**, 103-112.

**Wallenfang, M. R. and Seydoux, G.** (2000). Polarization of the anterior-posterior axis of *C. elegans* is a microtubule-directed process. *Nature* **408**, 89-92.

**Wicks, S. R., Yeh, R. T., Gish, W. R., Waterston, R. H. and Plasterk, R. H.** (2001). Rapid gene mapping in *Caenorhabditis elegans* using a high density polymorphism map. *Nat. Genet.* **28**, 160-164.

**Yong, W., Bao, S., Chen, H., Li, D., Sanchez, E. R. and Shou, W.** (2007). Mice lacking protein phosphatase 5 are defective in ataxia telangiectasia mutated (ATM)-mediated cell cycle arrest. *J. Biol. Chem.* **282**, 14690-14694.